

Evaluation of Crankshaft Properties: Mechanical Testing and Microscopic Analysis

Ioana GHIUȚĂ

Transilvania University of Brasov, Romania, ioana.ghiuta@unitbv.ro

Abstract

The crankshaft is a critical element of internal combustion engines, extensively utilized in automotive applications. Fatigue failure represents the most prevalent mechanism of crankshaft failure. The experimental analysis focused on investigating the properties and characteristics of the material used in manufacturing the shaft for the ARO 244 vehicle. This research aimed to comprehensively evaluate the material's performance under operational conditions by examining its chemical composition, microstructural features, and mechanical behaviour. By understanding these attributes, the study sought to assess the suitability of the material for ensuring the durability, strength, and reliability of the shaft during prolonged use. The vehicle was manufactured at Brasov, having in the moment of failure more than 400,000 kilometers. The samples were analysed from microscopic, chemical, and mechanical perspectives. From a mechanical standpoint, the samples were subjected to bending, torsion, compression and resilience.

Keywords

crankshaft, fracture failure, mechanical analysis

1. Introduction

On the current market there is a wide range of automobiles, both in terms of manufacturers and the performance of internal combustion engines and the comfort offered to future customers. However, the high cost represents a major disadvantage for manufacturers [1, 2]. Another major issue besides this is durability. Due to the high loads resulting from the operating cycle, the damage is represented by the forces that occur during the operating cycle. To have the highest possible efficiency, researchers focus on both the design and the materials used in their manufacture [1-4]. The researchers' vision for increasing engine performance, must comply with strict regulations on internal combustion engine emissions [5], multiple previous studies being conducted on the strategies of new internal combustion modes [6]. However, due to the late injection, there are a variety of increasing factors in terms of premature wear and more pronounced shocks of internal components in the operating system [7].

In engine operation, crankshafts are characterized as the heart of the engine, interconnecting a wide series of components in the operating cycle that transform fuel combustion into rotational motion. When a shaft is set in motion, by a torque due to the intensity of the explosion in the cylinder, the rotational movement around its axis is achieved, shear stresses are established in the direction perpendicular to its radius. The complementary shear stresses in the longitudinal plane of the crankshaft will cause a distortion of the structures through torsional vibration [8]. Torsional vibration depends on the radius of the crankshaft, the length of the crankshaft, the angle of rotation and the shear force. The failure of crankshafts has been characterized by excessive vibrations in the structure of the main/thrust bearing material [2, 8]. Silva F.S. has reported the investigation results of a vehicle crankshaft failure. In that study two damaged crankshafts from diesel vans, each of them having been in use for around 300,000 kilometers, were subjected to examination, through grinding, after their operational lifespan. The nearly imperceptible fractures were characterized by sharp edges and acted like knives. This was found to accelerate deterioration of the journal bearings and consequently causing damage to the journals themselves [9].

One particular investigation focused on the failure of a diesel engine crankshaft used in ARO 244 vehicle with an engine manufactured in Brasov. After approximately 400,000 km of operation, it failed,

causing major damage to the entire engine assembly. In this paper, the mechanical properties determined on a crankshaft were analysed, with the emphasis on determining the fracture of the part after a certain number of successive operating cycles. It is interesting to note that it is simultaneously subjected to a multiple succession of forces during a cycle.

2. Materials and Methods

Experimental research took place within the laboratories of the Research and Development Institute of the Transilvania University of Brasov, Faculty of Materials Science and Engineering. The samples were carefully collected and prepared in accordance with the specific requirements of each type of analysis. For each test, the specimens were shaped to meet the standards necessary for accurate results. This process involved precise cutting and polishing specific areas with defects on the crankshaft. These targeted sections were carefully selected to ensure that the analysis would focus on the material's behavior and performance in regions most affected by wear, stress, or structural weaknesses.

The microscopically investigated samples were chemically attacked with 10% Nital, with a holding time of 30 seconds, and then washed under a water jet and with ethyl alcohol, to eliminate traces of reagent from the surface of the piece, followed by drying by gently tapping on filter paper. In this way, the metallographic constituents of which the crankshaft material is made up were highlighted. The samples were analyzed using the Omnimet-Buehler Structural Analysis System, equipped with a Nikon microscope (with a resolution of up to 1000x) and appropriate software for quantitative structural analyses. The chemical composition of the material was determined using a Spectomax XF-BT Spectrometer, with a scintillation counter. The hardness test was performed with a Rockwell HRC Hardness Meter Mitutoyo 963, using a conical diamond indenter. The impact test was performed on different specimens with a "V" shaped notch to determine brittleness; specimens with a "U" shaped notch to determine toughness; specimens without a notch to determine impact bending. These tests were performed using a Charpy hammer, which allowed for the precise determination of the material's ability to absorb energy under impact. The mechanical properties, compression and torsion, were tested according to STAS SR EN ISO 527-1 on the Universal Testing Machine, model WDW-150S. This allows determinations and tests on non-standardized samples of mechanical properties, for a very wide temperature range (from -150 °C to 1250 °C). The test force is between 1 and 150 KN.

3. Results and Discussions

From a macroscopic point of view, it is observed that the shaft presents a fracture in the connecting rod crankpin area, around the oil lubrication hole (figure 1A).



Fig. 1. A) – Crankshaft; B) – Broken crankshaft; C) – Breakage detail
D) The appearance of the fracture surface

The fracture is ductile in nature due to the con-cup aspect it presents (figures 1B and 1C). Ductile fracture can occur when the temperature at which the part under test normally works increases. Ductile

fracture begins, following plastic deformations localized in the neck formation area in the case of a metallic material being subjected to traction, by the germination of microcracks whose density increases as the deformation increases. Microcrack germination occurs because of the blocking of dislocations in motion under the action of tangential stresses at the level of non-metallic inclusions or secondary phases (carbides in the case of unalloyed or alloyed steels) dispersed in the metallic matrix.

Ductile fracture is mainly caused by tangential stresses (also called shear failure) and is preceded by large plastic deformations, the appearance of the fracture surface being matte-fibrous (figure 1D). Ductile fracture occurs trans-crystallinely and has a relatively slow propagation speed.

If we look perpendicular to the fracture zone, the central area of the cup can be seen to have an apparently fibrous structure, as if the specimen had broken into a series of individual longitudinal fibers, each of which had constricted, reaching a point-like size, before rupture. If the rupture zone is sectioned longitudinally, the central crack has a jagged appearance. The outer cone of the fracture represents a highly localized shear zone. A very large local deformation occurs by the sliding of grains over each other and, because shear rupture propagates rapidly, compared to fibrous rupture, it is accompanied by significant local heating.

Microscopic analysis was performed on samples taken from the fracture area, to identify possible material defects that could have led to the crankshaft fracture. At low magnifications, namely 50x (figures 2a and 2b), a uniform structure is observed, formed by grains of similar shapes and sizes. The white (shiny) areas represent the uncorroded constituents, those on which the attack with 10% Nital had no effect. With increasing magnification, the structure of the material begins to be better defined, thus allowing the metallographic constituents to be differentiated.

Even at 100x magnification (figures 2c and 2d) it can be observed that the alloy is a eutectoid, namely a mechanical mixture of two (in this case) solid phases resulting from their simultaneous crystallization at constant temperature. This fact is observed more and more clearly at higher magnifications, namely, both in figures 2e and 2f, but especially in figures 2g and 2h. The eutectoid mixture is formed in this case from ferrite and cementite, thus resulting in pearlite. In its equilibrium state, pearlite is represented in the form of alternating ferrite and cementite lamellae, the appearance of the structure being comparable to a human fingerprint. From the point of view of homogeneity, it is observed that the material is homogeneous, ferrite and cementite being approximately uniformly distributed throughout the surface of both analyzed samples.

Chemical analysis was performed to determine the type of steel used in the manufacture of the crankshaft. For good accuracy of the results, according to the procedure, five measurements were performed on the same sample. This stage is also necessary to determine the homogeneity of the material; the higher the measurement values, the more homogeneous the material is. According to the values of the chemical analysis results, the steel grade from which the crankshaft is made could be 90VMn20 according to STAS 3611-88. This is a steel wear-resistant tool, and the limits imposed by the standard for this material are:

Table 1. Chemical composition of 90VMn20 (crankshaft material)

| C | Mn | Si | Cr | Ni | V | P |
|-------------|-------------|-------------|--------|--------|-------------|--------|
| 0.80 – 0.95 | 1.80 – 2.20 | 0.10 – 0.40 | ≤ 0.35 | ≤ 0.35 | 0.05 – 0.20 | ≤0.030 |

Mechanical hardness. The results of hardness tests presented in the table 2 indicate that the material shows good resistance against the action of a hard body penetrating its mass. This fact is also defining for the application for which it was intended, namely the crankshaft, which is constantly subjected to wear and the action of various forces on it.

Table 2. Mean results of hardness tests

| Samples | Sample 1 | Sample 2 |
|----------------|----------|----------|
| Hardness [HRC] | 63.8 | 63.9 |

The "V" notch specimens, figure 3, used to determine the toughness of the steel from which the crankshaft was made. The material is tough when it fractures as soon as its elastic limit is reached.

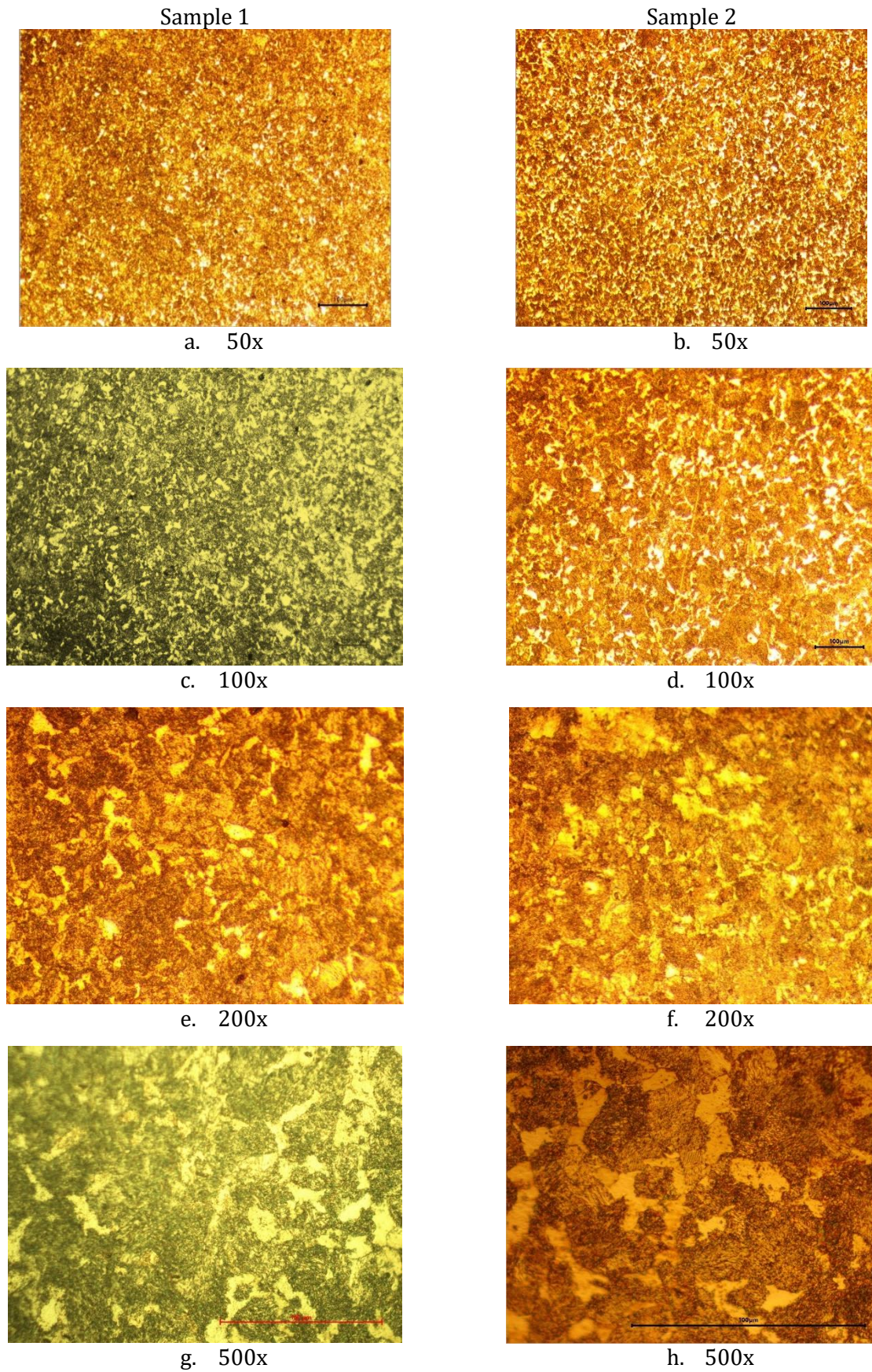


Fig. 2. Microstructures of sample at different magnifications

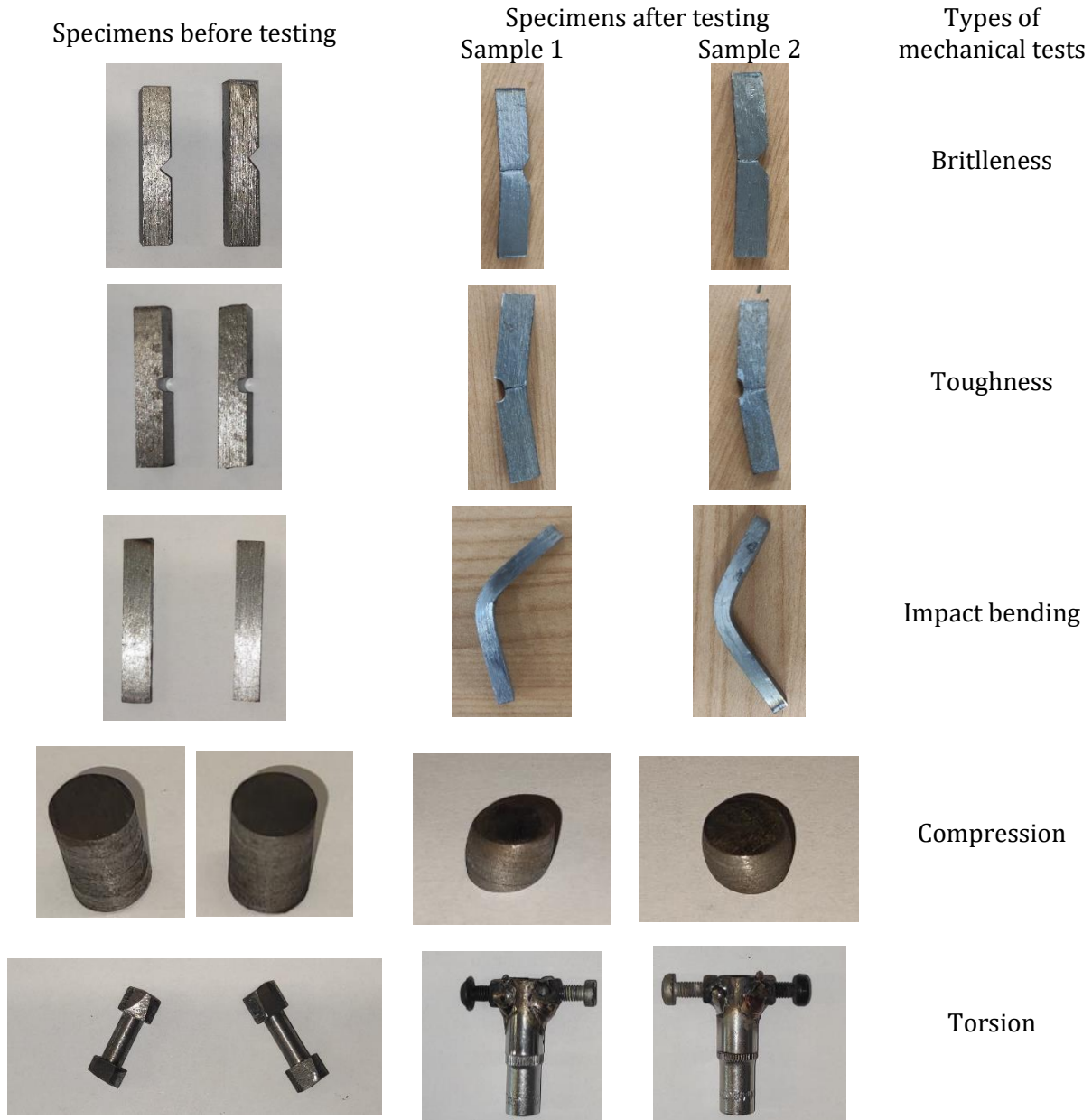


Fig. 3. Samples subjected to mechanical testing

Toughness is the opposite of ductility, so the material has a low resistance to crack propagation. Both in everyday life and in metallurgy, a material is tough when there is a low deformation at break, low strength and low breaking energy. Namely, when the brittle-ductile transition temperature is crossed, the elongation at break, strength and fracture energy decrease together.

To determine the values of brittleness resistance, equation (1) was used:

$$\sigma f = \frac{3FL}{2bh^2} \quad (1)$$

where h represents the thickness of the specimen, [mm]; b represents the width of the specimen, [mm]; σf represents the bending stress, [MPa]; F represents the force, [N]; L represents the distance between the supports, [mm] [10]. The resulting values are those in table 3.

Table 3. Calculated values of brittleness resistance

| Sample | Sample 1 | Sample 2 |
|----------------|----------|----------|
| Obtained value | 2.43 | 1.97 |

As can be seen both in the image in Figure 3 and Table 3, the sample 1 is more deformed, indicate a higher value). This may be due to the fact that the sample was taken from the same area as the one for the brittleness test. Figure shows the specimens used to determine the impact bending of the steel from which the crankshaft was made. Equation (1) was used to determine the values at which the samples bent, the values being presented in Table 4.

Table 4. Calculated values of impact bending resistance

| Sample | Sample 1 | Sample 2 |
|----------------|----------|----------|
| Obtained value | 2.28 | 2.30 |

Mechanical compression test. The compression test was performed on 3 samples in order to determine the resistance of the material from which the crankshaft was made, to the action of pressing forces.

| | | | | | | | |
|----------|------|----------------------|-------|----------|-------|----------------------|-------|
| Size(mm) | 9.9 | So(mm ²) | 76.98 | Size(mm) | 10.07 | So(mm ²) | 79.64 |
| Lo(mm) | 15.7 | Fbc(kN) | 78.86 | Lo(mm) | 15.85 | Fbc(kN) | 68.22 |
| Rbc(MPa) | 1025 | Fsc(kN) | 66.01 | Rbc(MPa) | 855 | Fsc(kN) | 62.47 |
| Rsc(MPa) | 855 | Fpc(kN) | 59.11 | Rsc(MPa) | 785 | Fpc(kN) | 57.62 |
| Rpc(MPa) | 770 | Ftc(kN) | 1.83 | Rpc(MPa) | 725 | Ftc(kN) | 3.03 |
| Rtc(MPa) | 24 | Ec(GPa) | 8.37 | Rtc(MPa) | 38 | Ec(GPa) | 6.26 |

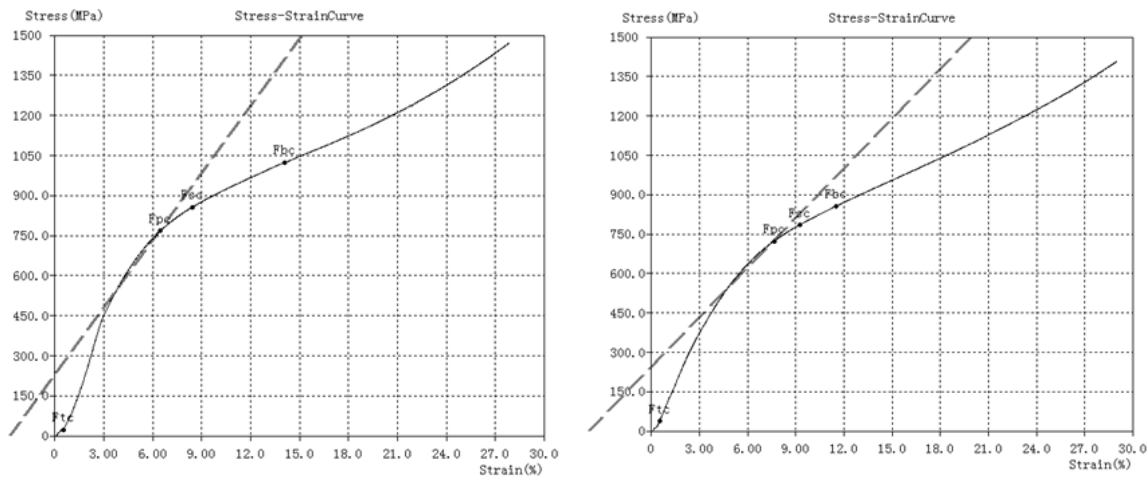


Fig. 4. Graphs of mechanical compression tests

| | | | | | | | |
|----------|----|----------------------|-------|----------|----|----------------------|-------|
| Size(mm) | 6 | So(mm ²) | 28.27 | Size(mm) | 6 | So(mm ²) | 28.27 |
| Lo(mm) | 10 | Fbc(kN) | 0.84 | Lo(mm) | 10 | Fbc(kN) | 1.46 |
| Rbc(MPa) | 30 | Fsc(kN) | / | Rbc(MPa) | 52 | Fsc(kN) | / |
| Rsc(MPa) | / | Fpc(kN) | 0.57 | Rsc(MPa) | / | Fpc(kN) | 0.73 |
| Rpc(MPa) | 20 | Ftc(kN) | 0.04 | Rpc(MPa) | 26 | Ftc(kN) | / |
| Rtc(MPa) | 1 | Ec(GPa) | 0.04 | Rtc(MPa) | / | Ec(GPa) | 0.04 |

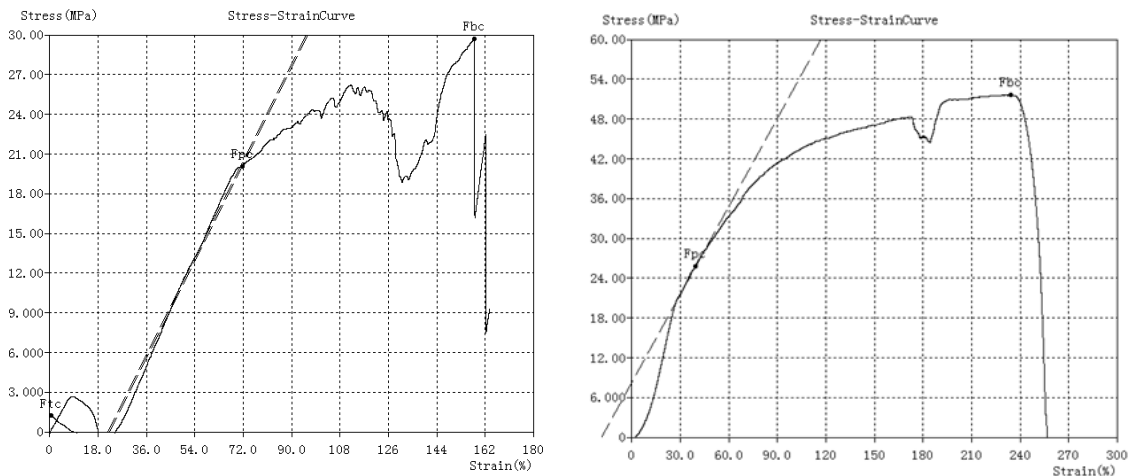


Fig. 5. Results of mechanical torsion tests

In figure 3 it can be seen even the samples that were subjected to the mechanical compression test. It can be noticed that they did not yield under the action of the applied force, but instead they underwent changes in terms of their shape, both presenting a barrel-shaped appearance. As can be seen from the graph presented in figure 4, regarding sample 1, it reaches the yield load at a value of 78.86 kN and sample 2 at a value of 68.22 kN.

Mechanical Torsion Test. The mechanical torsion test was performed on the samples, in order to analyze the behavior of the material in pure shear. The test was performed by rotating the samples to a certain degree, with a certain force until the material failed or broke. The rotational force of a torsion test was applied by fixedly attaching one end of the sample. Thus, one end of the sample under test was secured, while the other end was rotated and thus the sample was rotated around its axis. Rotational movement is possible at both ends of the sample, these being rotated in opposite directions.

The graph shown in figure 5 shows the torsion regime of specimen number one. In the case of this specimen, the tension mechanism (suffa) of the torsion machine failed due to the resistance opposed by the sample during the stress. The conclusion of this fact can be that the material presented a good torsion resistance.

4. Conclusions

The experimental research of this study was based on the metallographic, chemical and mechanical characterization of a crankshaft that failed during operation. Through macroscopic analysis, it was determined that the shaft failed due to the propagation of a crack that led to its breakage in the crankpin area. This area is prone to failure during operation due to the forces acting on it: - the connecting rod attachment area from the piston: area with stresses induced by the connecting rod-crank movement, friction, etc. - the area prone to the propagation of cracks that can be induced during the machining of the lubrication holes - the area prone to breakage due to temperature changes, etc.

Microscopic analysis revealed the existence of cracks, material defects in the breakage area, an aspect that indicates that the area was prone to failure during operation. The chemical attack highlighted the structure of the material from which the crankshaft was made, namely a eutectoid mixture of ferrite and cementite, hence pearlite (human fingerprint appearance). Through chemical analysis, it was determined that the steel grade from which the crankshaft is made could be 90VMn20 according to STAS 3611-88. This is a wear-resistant tool steel, an important aspect for the proposed area I hope to use. The mechanical tests to which the samples taken from the crankshaft were subjected demonstrated that those taken from the fracture area showed a different behavior compared to the others taken from neighboring areas. The general conclusion that can be drawn from this study is that the area where the breakage occurred was an area with material defects resulting either from manufacturing or from processing the finished part.

Acknowledgements

I would like to thank my colleague, Scientific Researcher II Mihai-Alin POP, for his valuable assistance with the testing process. His support and expertise were crucial to the success of this work.

References

1. Rațiu S.A., Mihon N.L., Armioni, M.D. (2024): *Overview on potential, opportunities and trends for internal combustion engines*. IOP Conference Series: Materials Science and Engineering, Vol. 1311, is. 1, art. 012052, <http://dx.doi.org/10.1088/1757-899X/1311/1/012052>
2. Popescu I. (2021): *Materiale utilizate în industria auto (Materials used in the automotive industry)*. Printech, ISBN 978-606-23-1217-6 (in Romanian)
3. Sadegh A.M., Worek W.M. (2018): *Marks' Standard Handbook for Mechanical Engineers*. 12th Edition. McGraw-Hill Education, ISBN 978-1259588501
4. Montazersadgh F.H., Fatemi A. (2007): *Stress analysis and optimization of crankshafts subject to dynamic loading*. A Final Project Report Submitted to the FIERF and American Iron and Steel Institute (AISI), University of Toledo, <https://www.yumpu.com/en/document/view/49009699/stress-analysis-and-optimization-of-crankshafts-subject-to-dynamic->

5. Awad O.I., Ma X., et al. (2020): *Particulate emissions from gasoline direct injection engines: A review of how current emission regulations are being met by automobile manufacturers*. Science of The Total Environment, eISSN 1879-1026, Vol. 718, art. 137302, <https://doi.org/10.1016/j.scitotenv.2020.137302>
6. Duan X., Lai M.C., Jansons M., Guo G., Liu J. (2021): *A review of controlling strategies of the ignition timing and combustion phase in homogeneous charge compression ignition (HCCI) engine*. Fuel, eISSN 1873-7153, Vol. 285, art. 119142, <https://doi.org/10.1016/j.fuel.2020.119142>
7. Xu H., Yankai L., Sjöberg M., Vuilleumier D., Ding C.P., Fushui L., Xiangrong L. (2019): *Impact of coolant temperature on piston wall-wetting and smoke generation in a stratified-charge DISI engine operated on E30 fuel*. Proceedings of the Combustion Institute, eISSN 1873-2704, Vol. 37, is. 4, pp. 4955-4963, <https://doi.org/10.1016/j.proci.2018.07.073>
8. Mendes A.S., Meirelles P.S., Zampieri D.E. (2008): *Analysis of torsional vibration in internal combustion engines: Modelling and experimental validation*. Proceedings of the Institution of Mechanical Engineers, Part K: Journal of Multi-body Dynamics, eISSN 2041-3068, Vol. 222, is. 2, pp. 155-178, <https://doi.org/10.1243/14644193JMBD126>
9. Silva F.S. (2003): *Analysis of a vehicle crankshaft failure*. Engineering Failure Analysis, eISSN 1873-1961, Vol. 10, is. 5, pp. 605-616, [http://dx.doi.org/10.1016/S1350-6307\(03\)00024-4](http://dx.doi.org/10.1016/S1350-6307(03)00024-4)
10. Matei S.C., Crişan A. (2020): *Compozite termoplastice. Compozite termorezistente (Thermoplastic composites. Thermosetting composites)*. Editura Universităţii Transilvania din Braşov, ISBN 978-6061912223 (in Romanian)